



A rare earth free magnesium alloy with exceptional thermal stability and enhanced mechanical properties

M. Elhami^a, M.A. Jabbareh^{a,b,*}, B. Korojy^a

^a Department of Materials Engineering, Hakim Sabzevari University, Sabzevar, Iran

^b Department of Materials Science and Engineering, Engineering Faculty, Ferdowsi University of Mashhad, Mashhad, Iran

ARTICLE INFO

Keywords:

Magnesium alloy
Multi-principal element alloy
Thermal stability
Intermetallic compounds

ABSTRACT

Mg-RE alloys are recognized as high-performance heat-resistant magnesium alloys, but the high cost of rare-earth elements has limited their applications. In this study, a cost-effective, heat-resistant multi-principal element magnesium alloy, $\text{Mg}_{80}\text{Al}_{10}\text{Cu}_5\text{Zn}_5$ (at.%), was developed. In the as-cast condition, the alloy exhibits a yield strength of 228 ± 6 MPa and an ultimate compressive strength of 477 ± 5 MPa, surpassing conventional heat-resistant Mg alloys. Following 96 h of heat exposure at 300 °C, the alloy exhibits desirable mechanical properties at ambient and high temperatures, indicating its exceptional thermal stability.

1. Introduction

The growing demand for lightweight materials in automotive, aerospace, and defense industries has driven significant interest in magnesium alloys, particularly cast variants, which constitute over 90 % of industrial applications [1]. Despite the advantages of Mg alloys their use remains limited due to low ambient-temperature strength [2] and poor thermal stability at elevated temperatures [3]. Efforts to overcome these limitations led to the development of heat-resistant Mg-RE alloys [4]. However, the high cost of RE elements limits the widespread adoption of these alloys, underscoring the need for cost-effective alternatives. Multi-principal element Mg alloys (Mg-MPEAs), with the concentration of each element in the range of 5–35 at.%, could be considered as possible alternatives due to their exceptional mechanical properties [5]. Despite their potential, Mg-MPEAs have remained unexplored and their thermal stability has not been systematically investigated. In this work, we designed a cost-effective $\text{Mg}_{80}\text{Al}_{10}\text{Cu}_5\text{Zn}_5$ (at. %) alloy using the MPEA concept. Microstructure, mechanical properties, and thermal stability of the alloy in as-cast and heat-exposed (300 °C, 96 h) conditions were investigated, offering insights into its potential as a cost-effective heat-resistant Mg alloy.

2. Materials and method

The $\text{Mg}_{80}\text{Al}_{10}\text{Cu}_5\text{Zn}_5$ alloy was prepared by melting commercially pure Al (99.9 %), Mg (99.8 %), Zn (99.9 %), and an Cu-20 wt%Al master

alloy in an electrical resistance furnace at 700 °C under argon shielding. The molten alloy was cast into a steel mold ($19 \times 8.5 \times 1$ cm) preheated to 200 °C. Chemical composition was verified via inductively coupled plasma (ICP) analysis, confirming $\text{Mg}_{80.3}\text{Al}_{9.7}\text{Cu}_{4.9}\text{Zn}_{5.1}$, closely matching the designed composition. Cylindrical samples ($\phi 6 \times 9$ mm) were extracted from the original plate using wire-cut EDM. A subset was heat-exposed at 300 °C for 96 h under argon atmosphere, followed by water quenching. Microstructural analysis employed optical microscopy (Olympus-GX51) and SEM (Zeiss-sigma 300 HV) equipped with EDS. Samples were prepared via standard grinding, polishing, and etching. Phase identification was performed using XRD (Xpert-Pro MPD) with a scanning range of 10° to 80°. Compression tests (Zwick /Roell Z250 device, 0.001 s^{-1} strain rate) were conducted on as-cast (AC) and heat-exposed (HE) samples in room temperature and 200 °C. Compressive properties averaged from three tests.

3. Results and discussion

Fig. 1 shows the optical microscope (OM) and scanning electron microscope (SEM) images of AC and HE alloys, along with their corresponding EDS maps. The OM image of the AC sample (Fig. 1(A)) exhibits a microstructure dominated by eutectic colonies surrounded by irregularly shaped particles (Point 1), with some polygonal particles (Point 2) dispersed throughout. The SEM image (Fig. 1(B)) further elucidates the eutectic structure, showing alternating layers of intermetallic compounds (Point 3) within the matrix phase (Point 4). EDS mapping and

* Corresponding author at: Department of Materials Engineering, Hakim Sabzevari University, Sabzevar, Iran.

E-mail address: m.jabbareh@hsu.ac.ir (M.A. Jabbareh).

<https://doi.org/10.1016/j.matlet.2025.138707>

Received 25 February 2025; Received in revised form 2 May 2025; Accepted 6 May 2025

Available online 8 May 2025

0167-577X/© 2025 Elsevier B.V. All rights are reserved, including those for text and data mining, AI training, and similar technologies.

point analysis (Fig. 1(E)) identify four distinct phases. A Mg-rich matrix, Al-rich eutectic regions, Cu-rich polyhedral particles, and Zn-rich irregular zones. XRD (Fig. 2) and EDS data confirm that the matrix is a magnesium solid solution, while the eutectic intermetallics correspond to $\text{MgAl}_{0.93}\text{Cu}_{1.07}$. The polygonal particles are MgCu_2 , and the irregular particles are AlMg_2Zn . Quantitative analysis (Fig. 1(F)), indicates that the $\text{MgAl}_{0.93}\text{Cu}_{1.07}$ phase constitutes $\sim 22\%$ of the microstructure of AC alloy, $\text{AlMg}_2\text{Zn} \sim 12\%$, and $\text{MgCu}_2 < 1\%$, totaling $\sim 35\%$ intermetallic content. After 96 h at 300°C (Fig. 1(C) and (D)), the MgCu_2 and AlMg_2Zn phases persist, but the AlMg_2Zn fraction decreases from $\sim 12\%$ to $\sim 8\%$ with particle sizes shrinking from $25\ \mu\text{m}^2$ to $12\ \mu\text{m}^2$. The eutectic structure stable, with no significant changes in other intermetallic phases.

Fig. 3(A) illustrates the compressive stress–strain curves for the $\text{Mg}_{80}\text{Al}_{10}\text{Cu}_5\text{Zn}_5$ alloy in both AC and HE conditions at room temperature and 200°C . At ambient temperature the AC alloy demonstrates a compressive yield strength (CYS) of $228 \pm 6\ \text{MPa}$ and ultimate compressive strength (UCS) of $477 \pm 5\ \text{MPa}$. When tested at 200°C , the AC sample shows a 9 % drop in CYS (207 MPa) and a 16 % reduction in UCS (398 MPa). After heat exposure, the CYS decreases further to $191 \pm 3\ \text{MPa}$ (16 % reduction), while the UCS remains unchanged ($476 \pm 3\ \text{MPa}$), accompanied by an increased fracture strain of $14.1 \pm 0.4\%$. At 200°C , the HE sample experiences a 15 % decline in CYS (194 MPa) and a 21 % decrease in UCS (374 MPa) compared to the AC sample at room temperature. Despite this, even at elevated temperatures, the $\text{Mg}_{80}\text{Al}_{10}\text{Cu}_5\text{Zn}_5$ alloy retains higher strength than conventional heat-resistant magnesium alloys (e.g., WE43, QE22, ZK60), as shown in Fig. 3(B), highlighting its potential for high-temperature applications.

Although the strength of the alloy is lower than that of Mg-MPEAs, the $\text{Mg}_{80}\text{Al}_{10}\text{Cu}_5\text{Zn}_5$ alloy offers superior ductility, with a fracture strain of $12.3 \pm 0.1\%$ —significantly higher than the $< 5\%$ typically seen in high-strength Mg-MPEAs (see [supplementary materials](#)). This enhanced ductility likely stems from its microstructure, particularly the

soft matrix phase ($\sim 65\ \text{vol}\%$), consistent with observations in other ductile Mg-MPEA systems [6].

The superior mechanical strength of the cast $\text{Mg}_{80}\text{Al}_{10}\text{Cu}_5\text{Zn}_5$ alloy can be attributed to the high volume fraction and intrinsic strength of its intermetallic phases [7]. The $\text{MgAl}_{0.93}\text{Cu}_{1.07}$ phase, which constitutes the largest volume fraction of intermetallic compounds in the alloy, possesses an elastic modulus of 201 GPa which is substantially higher than that of strengthening intermetallic phases in conventional magnesium alloys, such as $\text{Al}_{11}\text{RE}_3$ (64–115 GPa) [8] or Al_2RE compounds ($\sim 140\ \text{GPa}$) [9]. These intermetallic phases enhance mechanical properties through second-phase strengthening and load transfer reinforcement mechanisms [7]. Additionally, the Mg matrix contains $\sim 6\ \text{at.}\%$ Al and $2\ \text{at.}\%$ Zn, contributing solid-solution strengthening estimated at $\sim 40\ \text{MPa}$ via Labusch's model [10]. The eutectic structure plays a critical role in balancing strength and ductility [11], and improving thermal stability. Thermal stability of the eutectic structure is likely due to a low lattice misfit between the α -Mg matrix and $\text{MgAl}_{0.93}\text{Cu}_{1.07}$ phase, and thermodynamic stability of the constituent phases [12] which resist coarsening and hence maintain mechanical properties of the alloy after thermal exposure.

The observed reduction in strength after heat exposure can be attributed to the diminished volume fraction of intermetallic compounds in the HE alloy, which weakens second-phase strengthening mechanisms [7]. While the improvement in elongation following thermal exposure (or in high temperatures) can be rationalized by the microstructural evolution observed in the alloy. The reduction in grain boundary (GB) wetting—evidenced by the decreased volume fraction and size of the AlMg_2Zn phase—suggests a transition toward incomplete wetting conditions. Such a transition likely alters stress distribution at grain boundaries, as discontinuous wetting phases are less prone to act as preferential crack initiation sites compared to continuous GB films [13]. This microstructural refinement may enhance ductility by promoting more homogeneous deformation, while the retained

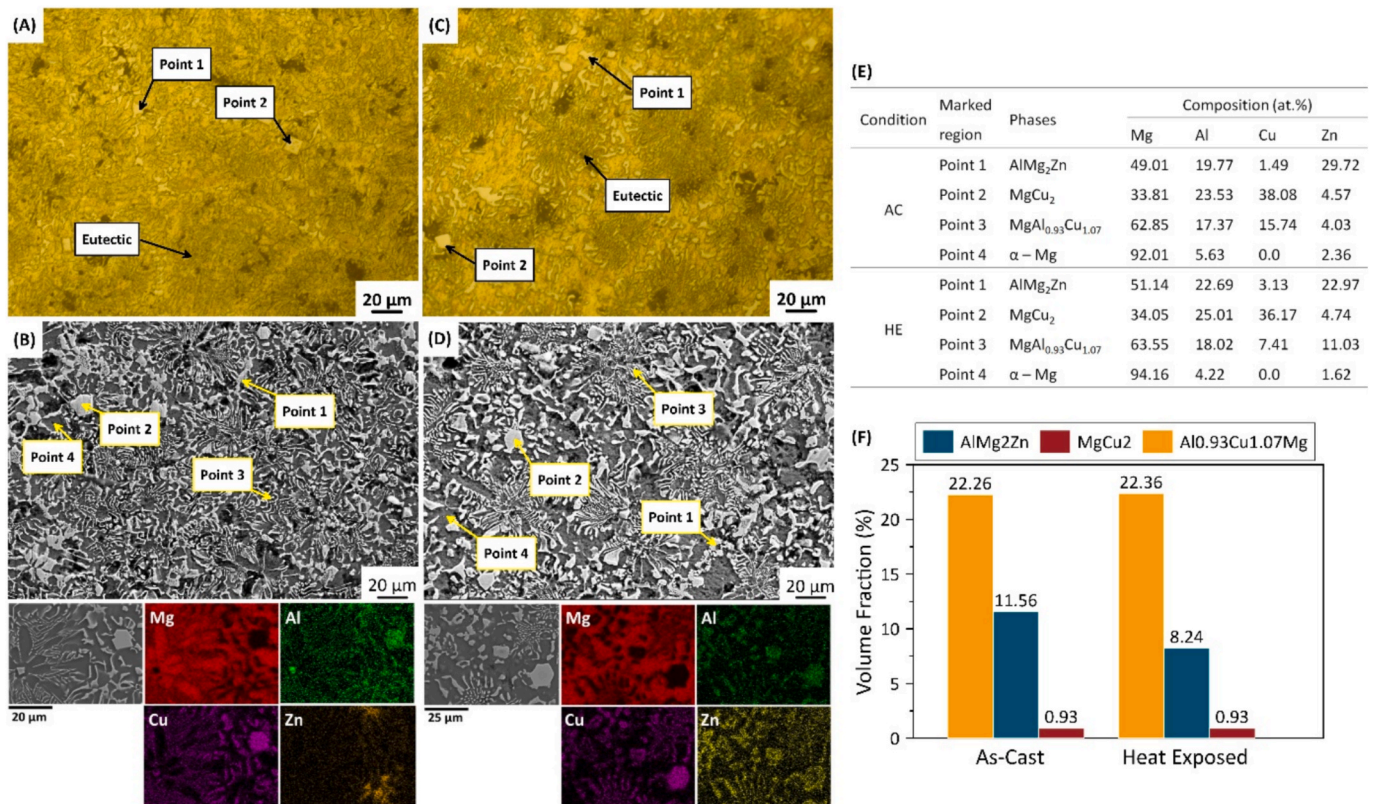


Fig. 1. (A and C) Optical and (B and D) SEM images showing the microstructure of as-cast (A and B) and heat-exposed (C and D) $\text{Mg}_{80}\text{Al}_{10}\text{Cu}_5\text{Zn}_5$ alloy. (E) EDS analysis results of identified phases. (F) Quantitative volume fraction of intermetallic compounds.

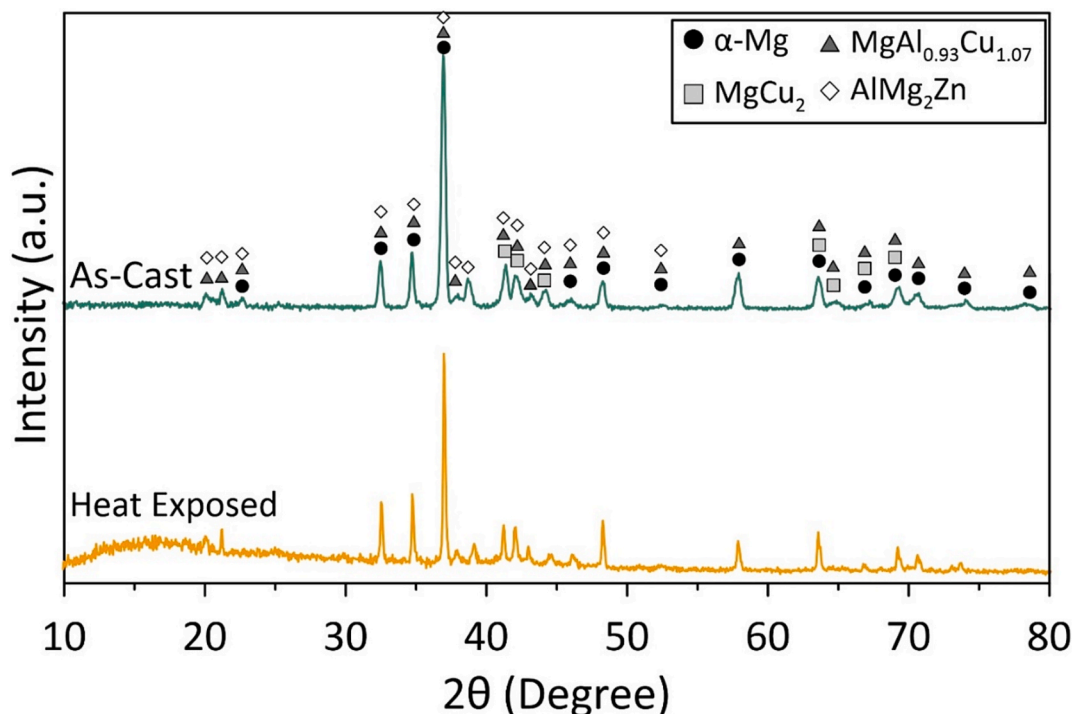


Fig. 2. XRD patterns of AC and HE samples.

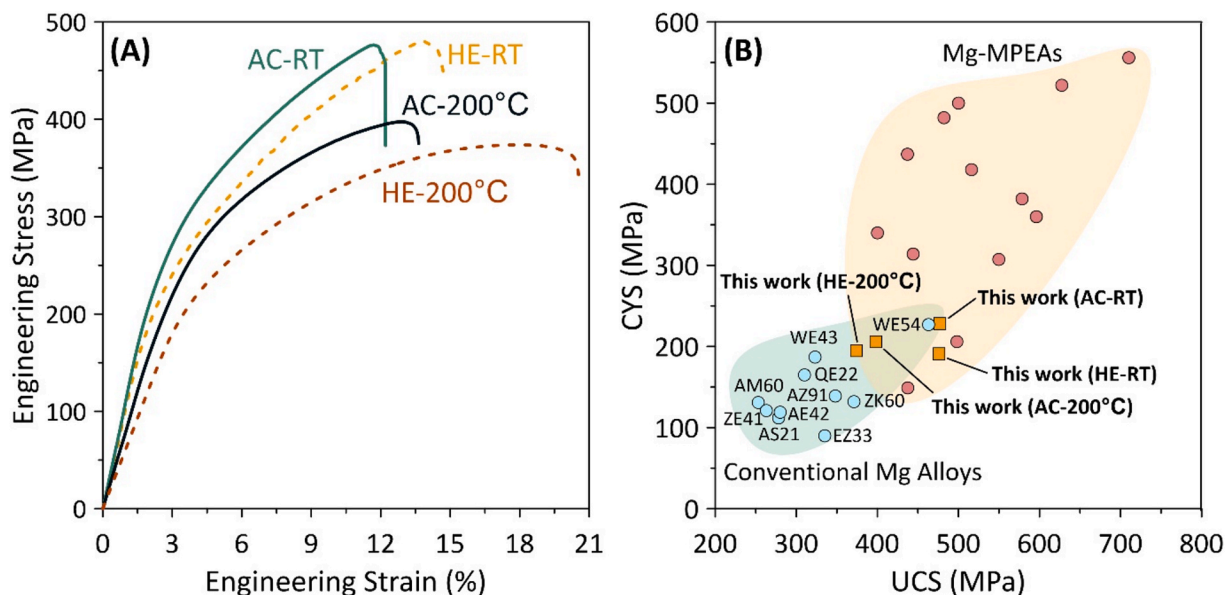


Fig. 3. (A) Compressive stress–strain curves of as-cast and heat-exposed alloys. (B) Comparison of CYS and UCS of $\text{Mg}_{80}\text{Al}_{10}\text{Cu}_5\text{Zn}_5$ with conventional heat resistant Mg alloys as well as multi-principal element Mg alloys. (All data given in supplementary materials).

intermetallic phases continue to provide strengthening via dispersion hardening [14].

4. Conclusion

In this study, the $\text{Mg}_{80}\text{Al}_{10}\text{Cu}_5\text{Zn}_5$ alloy was developed and evaluated for its mechanical properties and thermal stability. The as-cast alloy demonstrated superior compressive yield strength and ultimate compressive strength, compared to conventional magnesium alloys. After 96 h of heat exposure at 300 °C, the alloy retained significant mechanical properties, in ambient temperature and 200 °C, highlighting

its exceptional thermal stability. Importantly, the alloy achieves this performance without the use of expensive elements, making it a cost-effective alternative to conventional heat-resistant Mg alloys. The balanced combination of strength, ductility, and thermal stability positions the $\text{Mg}_{80}\text{Al}_{10}\text{Cu}_5\text{Zn}_5$ alloy as a promising candidate for structural applications in industries such as automotive and aerospace.

CRediT authorship contribution statement

M. Elhami: Writing – original draft, Methodology, Investigation. **M. A. Jabbareh:** Writing – review & editing, Supervision,

Conceptualization. **B. Korojy**: Writing – review & editing, Resources, Methodology.

Declaration of Generative AI and AI-assisted technologies in the writing process

During the preparation of this work the authors used *DeepSeek* in order to improve the readability and summarizing the text to less than 2000 words. After using this tool the authors reviewed and edited the content as needed and take full responsibility for the content of the published article.

Funding

This research did not receive any specific grant from funding agencies in the public, commercial, or not-for-profit sectors.

Declaration of competing interest

The authors declare that they have no known competing financial interests or personal relationships that could have appeared to influence the work reported in this paper.

Appendix A. Supplementary data

Supplementary data to this article can be found online at <https://doi.org/10.1016/j.matlet.2025.138707>.

Data availability

Data will be made available on request.

References

- [1] F. Sanling, L. Quanan, J. Xiaotian, Z. Qing, C. Zhi, L. Wenjian, Review on research and development of heat resistant Magnesium alloy, in: Proc. 2012 Int. Conf. Mech. Eng. Mater. Sci., 2012, pp. 611–614. doi: 10.2991/mems.2012.179.
- [2] J. Song, J. Chen, X. Xiong, X. Peng, D. Chen, F. Pan, Research advances of magnesium and magnesium alloys worldwide in 2021, J. Magnes. Alloy. 10 (2022) 863–898, <https://doi.org/10.1016/j.jma.2022.04.001>.
- [3] A.A. Luo, Recent magnesium alloy development for elevated temperature applications, Int. Mater. Rev. 49 (2004) 13–30, <https://doi.org/10.1179/095066004225010497>.
- [4] H. Yang, W. Xie, J. Song, Z. Dong, Y. Gao, B. Jiang, F. Pan, Current progress of research on heat-resistant Mg alloys: a review, Int. J. Miner. Metall. Mater. 31 (2024) 1406–1425, <https://doi.org/10.1007/s12613-023-2802-7>.
- [5] R. Li, G. Geng, Y. Zhang, Recent progress in lightweight high-entropy alloys, MRS Commun. 13 (2023) 740–753, <https://doi.org/10.1557/s43579-023-00405-7>.
- [6] Z. Gu, Y. Zhou, Q. Dong, G. He, J. Cui, J. Tan, X. Chen, B. Jiang, F. Pan, J. Eckert, Designing lightweight multicomponent magnesium alloys with exceptional strength and high stiffness, Mater. Sci. Eng. A 855 (2022) 143901, <https://doi.org/10.1016/j.msea.2022.143901>.
- [7] F. Wang, N. Dang, J. Chen, J. Li, T. Hu, W. Xiao, R. Zheng, V. Ji, C. Ma, The microstructural features and strengthening mechanisms of Mg-Al-Zn-Ca-(RE) extruded alloys having high-volume fractions of second-phase particles, Mater. Sci. Eng. A 868 (2023) 144765, <https://doi.org/10.1016/j.msea.2023.144765>.
- [8] T. Fan, L. Lin, H. Liang, Y. Ma, Y. Tang, T. Hu, Z. Ruan, D. Chen, Y. Wu, First-principles study of the structural, mechanical and thermodynamic properties of Al11RE3 in aluminum alloys, Crystals 13 (2023) 347.
- [9] X. Feng, X. Wang, C. Xu, H. Shi, X. Li, X. Hu, Z. Lu, G. Fan, Unveiling the microstructural features during compression of a large volume of Al2RE phases, Materials (basel). 17 (2024) 4784.
- [10] R. Labusch, Statistical theories of solid solution hardening, Acta Metall. 20 (1972) 917–927.
- [11] Q. Wu, Z. Wang, T. Zheng, D. Chen, Z. Yang, J. Li, J. Jung Kai, J. Wang, A casting eutectic high entropy alloy with superior strength-ductility combination, Mater. Lett. 253 (2019) 268–271, <https://doi.org/10.1016/j.matlet.2019.06.067>.
- [12] M. Wang, Y. Lu, J. Lan, T. Wang, C. Zhang, Z. Cao, T. Li, P.K. Liaw, Lightweight, ultrastrong and high thermal-stable eutectic high-entropy alloys for elevated-temperature applications, Acta Mater. 248 (2023) 118806, <https://doi.org/10.1016/j.actamat.2023.118806>.
- [13] B. Straumal, K. Tsoy, A. Druzhinin, V. Orlov, N. Khrapova, G. Davdian, G. Gerstein, A. Straumal, Coexistence of intermetallic complexions and bulk particles in grain boundaries in the ZEK100 alloy, Metals (Basel) 13 (2023) 1407, <https://doi.org/10.3390/met13081407>.
- [14] B. Straumal, N. Khrapova, A. Druzhinin, K. Tsoy, G. Davdian, V. Orlov, G. Gerstein, A. Straumal, Grain boundary wetting transition in the Mg-based ZEK 100 alloy, Crystals 13 (2023) 1538, <https://doi.org/10.3390/cryst13111538>.